Radiotherapy and Oncology 117 (2015) 83–90

Contents lists available at ScienceDirect

Radiotherapy and Oncology

journal homepage: www.thegreenjournal.com

Head and neck guidelines

CT-based delineation of organs at risk in the head and neck region: DAHANCA, EORTC, GORTEC, HKNPCSG, NCIC CTG, NCRI, NRG Oncology and TROG consensus guidelines

Charlotte L. Brouwer [a,*,1], Roel J.H.M. Steenbakkers [a,1], Jean Bourhis [b], Wilfried Budach [c], Cai Grau [d], Vincent Grégoire [e], Marcel van Herk [f], Anne Lee [g], Philippe Maingon [h], Chris Nutting [i], Brian O'Sullivan [j], Sandro V. Porceddu [k], David I. Rosenthal [l], Nanna M. Sijtsema [a], Johannes A. Langendijk [a]

[a] University of Groningen, University Medical Center Groningen, Department of Radiation Oncology, Groningen, The Netherlands; [b] Department of Radiation Oncology, Centre Hospitalier Universitaire Vaudois, Lausanne, Switzerland[2]; [c] Department of Radiation Oncology, University Hospital Düsseldorf, Germany; [d] Department of Oncology, Aarhus University Hospital, Denmark[3]; [e] Cancer Center and Department of Radiation Oncology, Clinical and Experimental Research Institute, Université Catholique de Louvain, Cliniques Universitaires St-Luc, Brussels, Belgium[4]; [f] Christie Hospital and University of Manchester, Manchester, UK; [g] Department of Clinical Oncology, The University of Hong Kong (Shenzhen) Hospital, China[5]; [h] Department of Radiation Oncology, Centre Georges-François Leclerc, Dijon, France[6]; [i] Department of Radiation Oncology, Royal Marsden Hospital and Institute of Cancer Research, London, UK[7]; [j] Department of Radiation Oncology, Princess Margaret Hospital, University of Toronto, Canada[8]; [k] Cancer Services, Princess Alexandra Hospital, University of Queensland, Brisbane, Australia[9]; and [l] Department of Radiation Oncology, The University of Texas M. D. Anderson Cancer Center, Houston TX, USA[10]

ARTICLE INFO

Article history:
Received 17 July 2015
Accepted 29 July 2015
Available online 13 August 2015

Keywords:
Head and neck
Organs at risk
Interobserver variability
Consensus delineation guidelines

ABSTRACT

Purpose: The objective of this project was to define consensus guidelines for delineating organs at risk (OARs) for head and neck radiotherapy for routine daily practice and for research purposes.
Methods: Consensus guidelines were formulated based on in-depth discussions of a panel of European, North American, Asian and Australian radiation oncologists.
Results: Twenty-five OARs in the head and neck region were defined with a concise description of their main anatomic boundaries. The Supplemental material provides an atlas of the consensus guidelines, projected on 1 mm axial slices. The atlas can also be obtained in DICOM-RT format on request.
Conclusion: Consensus guidelines for head and neck OAR delineation were defined, aiming to decrease interobserver variability among clinicians and radiotherapy centers.

In recent decades, the quality of radiotherapy imaging, planning and delivery has improved markedly. To fully utilize the benefits of these new technologies in radiation oncology practice, consistent delineation of targets and OARs has become increasingly important. However, delineation accuracy of targets and OARs is limited by interobserver and trial protocol variability. By reducing this variability, the generalizability and clinical utility of Tumor Control Probability (TCP) and Normal Tissue Complication Probability (NTCP) models in routine practice can be improved. To reduce treatment variations among clinicians and radiotherapy departments in the delineation of target volumes, guidelines for the delineation of the neck node levels for head and neck tumors have been developed [1]. The interobserver variability in the delineation of head and neck OARs is similar to the variation in the delineation of target volumes [2].

OAR delineation guidelines vary widely between publications and authors, resulting in inconsistent dose–volume reporting [3]. These inconsistencies hamper the comparison of dose–volume effect relationships as reported in studies using different delineation protocols [3]. We propose that both daily clinical practice and future multi-institutional clinical trials will benefit from improved consistency in delineation guidelines for OARs.

* Corresponding author.
[1] These authors contributed equally.
[2] Representing the Radiotherapy Oncology Group for Head and Neck (GORTEC).
[3] Representing Danish Head and Neck Cancer Group (DAHANCA).
[4] Representing the Head and Neck Cancer Group of the European Organisation for Research and Treatment of Cancer (EORTC).
[5] Representing the Hong Kong Nasopharyngeal Cancer Study Group (HKNPCSG).
[6] Representing the Radiation Oncology Group of the European Organisation for Research and Treatment of Cancer (EORTC).
[7] Representing the National Cancer Research Institute (NCRI).
[8] Representing the National Cancer Institute of Canada Clinical Trials Group (NCIC CTG).
[9] Representing the Trans Tasman Radiation Oncology Group (TROG).
[10] Representing the NRG Oncology Group.

http://dx.doi.org/10.1016/j.radonc.2015.07.041
0167-8140/

Therefore, the aim of this project was twofold: (1) to attain international consensus on the definition and delineation of OARs for head and neck radiotherapy and (2) to present consensus guidelines for CT-based delineation of a set of OARs in the head and neck region that are considered most relevant for radiotherapy practice.

Methods

To reach consensus on OAR guidelines, a panel of experts in the field of head and neck radiation oncology was established (WB, CG, VG, AL, PM, CN, JB, SP, DIR, BOS, JAL). The panel consisted of representatives from Europe, North America, Australia/New Zealand and Asia and members of the cooperative groups DAHANCA, EORTC, GORTEC, HKNPCSG, NCIC CTG, NCRI, NRG Oncology and TROG. For the purpose of this project, a number of group meetings were held during international conferences.

First, the panel agreed on an OAR set considered relevant for the most common acute and late side effects of head and neck radiotherapy. We did not discuss dose–volume effects or side effects for the OAR set in this paper, but focussed on a concise description of consensus guidelines for delineation.

Second, each member of the panel delineated the OARs in a CT set from one patient without any predefined guidelines. The CT images (2 mm slice thickness) were made with the patient in a supine position on a multidetector-row spiral CT scanner (Somatom Sensation Open, 24 slice configuration; Siemens Medical Solutions, Erlangen, Germany). The delineation environment used is dedicated to study interobserver variability [4]. Subsequently, the outcome of this procedure was presented to and discussed with the experts in order to identify the most prevalent inconsistencies and to formulate consensus guidelines.

Finally, consensus delineations were depicted on axial CT slices of an atlas of head and neck anatomy with 1 mm slice thickness. The CT images were registered with T2-weighted MRI images of the same anatomy for clarification. Since multimodal imaging is not the general standard at present, the atlas description was based on CT only.

Results

After the panel delineated the proposed OAR set (Fig. 1), variability in delineation for each OAR was discussed. Subsequently, the panel agreed on consensus definitions for each OAR and formulated the final consensus guidelines for the following 25 head-and-neck OARs:

Anterior segment of the eyeball

The anterior segment of the eyeball consists of the structures ventral from the vitreous humor, including the cornea, iris, ciliary body, and lens.

Posterior segment of the eyeball

The posterior segment of the eyeball is located posteriorly to the lens, and consists of the anterior hyaloid membrane and all of the posterior optical structures including the vitreous humor, retina, and choroid. The optic nerve is excluded from this contour. The entire retina is included in the posterior segment of the eyeball.

Lacrimal gland

The lacrimal gland is located superolateral to the eye and lies within the preseptal space.

The gland is molded at its inferomedial aspect to the globe, giving it a concave outline. The gland can be visualized on CT by its location partly encased in the bone and enveloped in low-density fat.

Parotid glands

The parotid glands were delineated according to previously published guidelines [5]. In these guidelines the retromandibular vein is included in the parotid gland contour, since it is difficult to discriminate it from the parotid gland tissue in non-contrast enhanced CT images. Anatomic borders are listed in Table 1. The use of a planning CT with intravenous contrast is however strongly recommended to be able to distinguish the extension of the glands from its surroundings.

Submandibular glands

The submandibular glands were delineated according to previous published guidelines [5]. Anatomic borders are listed in Table 1.

Extended oral cavity

The delineation of the extended oral cavity was based partly on Hoebers et al. [6]. For the sake of simplicity and consistency, the extended oral cavity structure was defined posterior to the internal arch of the mandible and maxilla. The mucosa anterior to the mandible and maxilla is included in the contour of the lips, and the mucosa lateral to the mandible and maxilla is included in the buccal mucosa (see next items and Fig. 3). Anatomic boundaries of the extended oral cavity contour are listed in Table 1.

For research purposes, the extended oral cavity can be subdivided into oral tongue and anterior oropharynx, by drawing a vertical line from the posterior hard palate to the hyoid (circumvallate line).

Buccal mucosa

The buccal mucosa is defined according to the borders listed in Table 1.

Lips

The lip contour extends from the inferior margin of the nose to the superior edge of the mandibular body. The lip contour was defined to include the lips as well as the inner surface of the lips (for delineation details concerning inner surface of the lips refer to Van de Water et al. [5]). Detailed anatomic boundaries of the lip contour are listed in Table 1.

Mandible

The mandible was defined as the entire mandible bone, without teeth. The use of CT bone view settings is recommended.

Cochlea

The cochlea is embedded in the temporal bone, located lateral to the internal auditory meatus, which can best be recognized in CT bone view settings (Fig. 2).

Pharyngeal constrictor muscles (PCM)

For the delineation of the PCM, many delineation guidelines are available in the literature. These are particularly variable regarding the cranial and caudal demarcation [3,7]. For the sake of simplicity and reproducibility, we defined the PCM as a single OAR. The cranial border was defined as the caudal tip of pterygoid plates (according to previous studies [7–12]), and the caudal border as the lower edge of the cricoid cartilage (similar to previous studies [8–12]). For pragmatic reasons, a thickness of 3 mm was assumed (Fig. 3).

For research purposes, the PCM may be further subdivided [7,13].

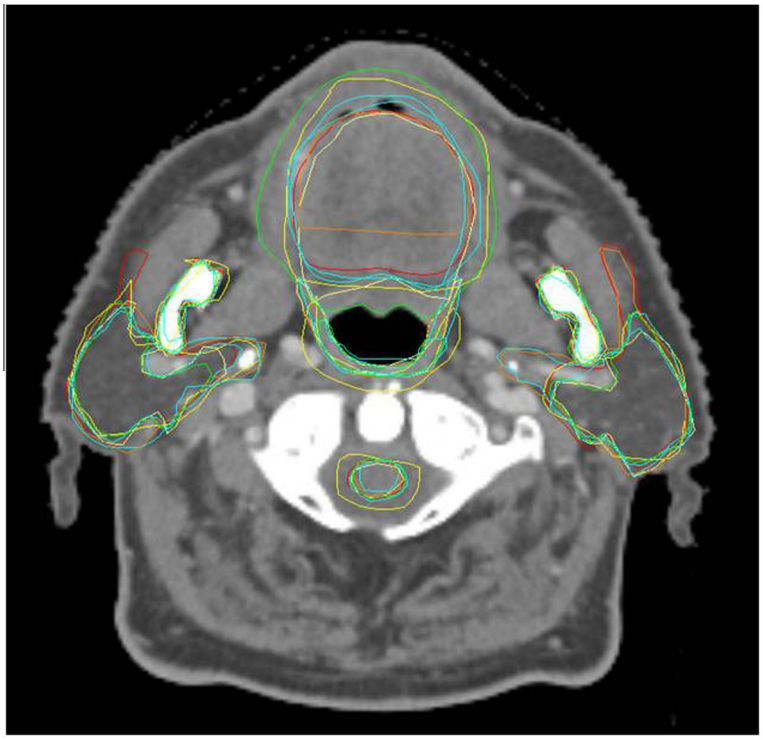

Fig. 1. Delineation results of 7 members of the panel for the parotid glands, spinal cord, pharyngeal constrictor muscles and the oral cavity, projected on an axial CT slice.

Supraglottic larynx

The supraglottic larynx is delineated according to Christianen et al. [7]. Anatomic borders are listed in Table 1. An axial slice of the supraglottic larynx is depicted in Fig. 4a.

Glottic area

We decided to define the glottic area structure, including the vocal cords and paraglottic fat. Air should be excluded from the contour. Cranial, caudal and posterior borders can be found in Table 1. An axial slice of the glottic area is depicted in Fig. 4b.

Arytenoids

The arytenoids (or arytenoids cartilage) are defined as a separate structure. The base (caudal edge) of each arytenoid is broad for articulation with the cricoid cartilage. The apex (cranial edge) is pointed.

Cricopharyngeal inlet

The crico-pharyngeal inlet represents the transition from the PCM to the cervical esophagus (Table 1). An axial slice of the crico-pharyngeal inlet is depicted in Fig. 4c.

Cervical esophagus

The cervical esophagus starts 1 cm caudal to the lower edge of the cricoid cartilage, and ends at the caudal edge of C7 (Table 1). An axial slice of the cervical esophagus is depicted in Fig. 4d.

Brachial plexus

It is difficult to localize the brachial plexus on CT. Anatomical borders are listed in Table 1, and a step-by-step technique, based on the guideline of Hall et al. [14], can be found in Supplemental material II.

Thyroid gland

The thyroid gland has two connected lobes and is located below the thyroid cartilage. It has considerable contrast compared to its surrounding tissues.

Brain

The delineation of the brain includes brain vessels, and excludes the brainstem. CT bone settings are recommended. In the case of nasopharyngeal cancer, a subdivision of brain structures could be made, i.e. delineation of the hippocampus and temporal lobe with the use of a brain atlas [15,16].

Brainstem

The cranial border of the brainstem was defined as the bottom section of the lateral ventricles, the caudal border as the tip of the dens of C2 (cranial border of the spinal cord). MRI is recommended for delineation of the brainstem. The bottom section of the lateral ventricles is clearly visible on both CT and MRI.

For research purposes, the brainstem could be further subdivided, for example according to Kocak-Uzel et al. [17].

Pituitary gland

The pituitary gland is a very small OAR, which in general cannot be identified easily on CT. Alternatively, however, the inner part of the sella turcica can be used as surrogate anatomical bony structure. The borders of the pituitary gland can be defined best in the sagittal view.

Optic chiasm

The optic chiasm is located in the subarachnoid space of the suprasellar cistern. Typically, it is located 1 cm superior to the pituitary gland, located in the sella turcica. MRI is recommended for

Table 1
Organs at risk with specification of anatomic boundaries. Ant. = anterior, post. = posterior, lat. = lateral, med. = medial, m. = muscle.

Organ at risk	Remarks	Anatomic boundaries					
		Cranial	Caudal	Anterior	Posterior	Lateral	Medial
Parotid gland	Include carotid artery, retromandibular vein and extracranial facial nerve.	External auditory canal, mastoid process	Post. part submandibular space	Masseter m., post. border mandibular bone, med. and lat. pterygoid m.	Ant. belly sternocleidomastoid m., lat. side post. belly of the digastric m. (posterior-medial)	Subcutaneous fat, platysma	Post. belly of the digastric m., styloid process, parapharyngeal space
Submandibular gland		Med. pterygoid m., mylohyoid m.	Fatty tissue	Lat. Surface mylohyoid m., hyoglossus m.	Parapharyngeal space, sternocleidomastoid m.	Med. surface med. pterygoid m., med. surface mandibular bone, platysma	Lat. surface mylohyoid m., hyoglossus m., superior and middle pharyngeal constrictor m., anterior belly of the digastric m.
Extended oral cavity	Posterior to mandible and maxilla, no inner surface of the lips	Hard palate mucosa and mucosal reflections near the maxilla	The base of tongue mucosa and hyoid posteriorly and the mylohyoid m. and ant. belly of the digastric m. anteriorly	Inner surface of the mandible and maxilla	Post. borders of soft palate, uvula, and more inferiorly the base of tongue	Inner surface of the mandible and maxilla	
Lips		Hard palate (lateral), anterior nasal spine (at the midline)	Lower edge teeth sockets, cranial edge mandibular body	Outer surface of the skin	Mandibular body, teeth, tongue, air (if present)	Depressor anguli oris m., buccinator m., levator anguli oris m./risorius m. Buccinator	
Buccal mucosa		Bottom of maxillary sinus	Upper edge teeth sockets	Lips, teeth	Med. pterygoid m.	Buccal fat	Outer surface of the mandible and maxilla, oral cavity/base of tongue/soft pallate
Pharyngeal constrictor muscle	Thickness ~3 mm	Caudal tips of pterygoid plates	Caudal edge of arytenoid cartilages	Superior: hamulus of pterygoid plate; mandibula; base of tongue; pharyngeal lumen. Middle: base of tongue; hyoid. Inferior: soft tissue of supraglottic/glottic larynx	Prevertebral muscle	Superior: medial pterygoid muscle. Middle: greater horn of hyoid bone. Inferior: superior horn of thyroid cartilage	
Supraglottic larynx		Tip of epiglottis	Cranial edge of arytenoid cartilages	Hyoid bone, pre-epiglottic space, thyroid cartilage	Inferior PCM, pharyngeal lumen	Thyroid cartilage	Pharyngeal lumen (lumen excluded)
Glottic area		Cranial edge of arytenoid cartilages	Caudal edge of ant. part of thyroid cartilage		Cricoid, anterior border arytenoids		
Crico-pharyngeal inlet		Caudal edge of arytenoid cartilages	1 cm caudal to the lower edge of the cricoid cartilage	Tracheal lumen	Vertebral body		
Cervical esophagus		1 cm caudal to the lower edge of the cricoid cartilage	Caudal edge of C7				
Brachial plexus	If the brachial plexus is wrapped around the vascular bundle on the most inferior slices, the vascular structure is included in the contour	Cranial border of C5, vertebral body	Cranial border of T3, vertebral body	Post. border of: anterior scalene m., subclavian artery, axillary vein	Ant. border of: middle scalene m., seratus anterior m., subscapularis m.	Lat. border of: ant. and middle scalene m., pectoralis major, teres major	Inter vertebral foramen (bony vertebral body), lat. border of 1st rib

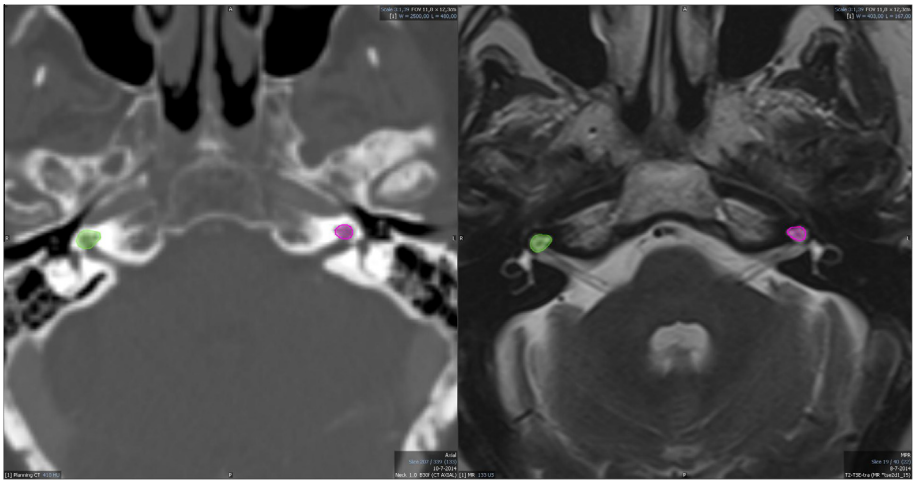

Fig. 2. Delineation of the cochlea in CT bone settings (left), matched to MRI-T2 (right).

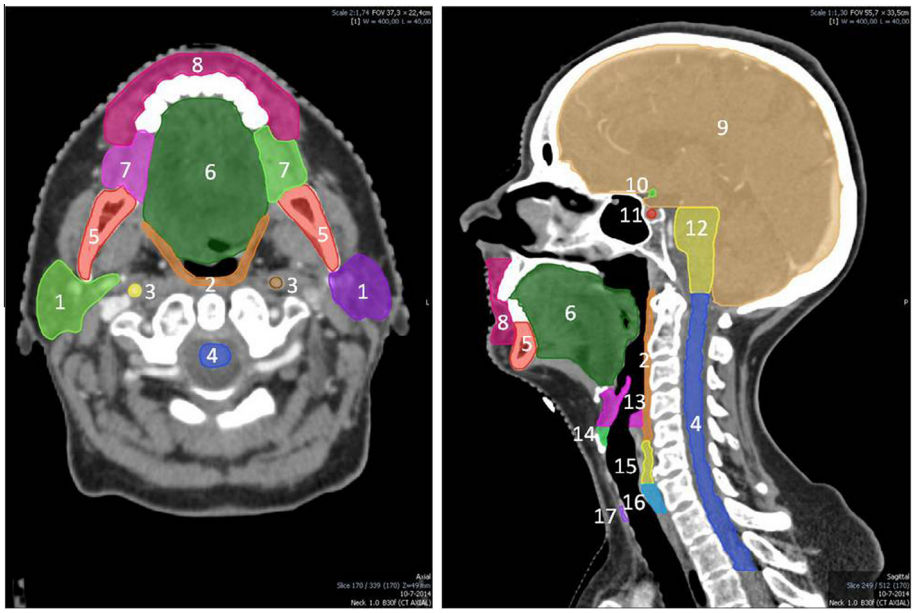

Fig. 3. Axial (left) and sagittal (right) view of the consensus delineations of the parotid glands (1), pharyngeal constrictor muscles (2), carotid arteries (3), spinal cord (4), mandible (5), extended oral cavity (6), buccal mucosa (7), lips (8), brain (9), chiasm (10), pituitary gland (11), brainstem (12), supraglottic larynx (13), glottic area (14), cricopharyngeal inlet (15), cervical esophagus (16) and thyroid (17). (For the full atlas, the reader is referred to the Supplemental material.)

delineation of the optic chiasm. It is demarcated laterally by the internal carotid arteries and inferiorly to the third ventricle (Fig. 5) [19,20].

Optic nerve

The optic nerve is usually 2–5 mm thick and in general is clearly identifiable on CT [20]. It has to be contoured all the way from the posterior edge of the eyeball, through the bony optic canal to the optic chiasm. MRI is recommended for a better delineation of the optic nerve, at least close to the optic chiasm.

Spinal cord

The spinal cord is delineated as the true spinal cord, not the spinal canal. The cranial border was defined at the tip of the dens of C2 (the lower border of the brainstem), and the caudal border at the upper edge of T3. With caudally located tumours or lymph node areas, we advise extending the spinal cord contours by at least 5 cm caudal to the PTV.

Carotid arteries

The carotid arteries include the common and internal carotid artery (external carotid artery was omitted). The left and right common carotid arteries follow the same course with the exception of their origin. The right common carotid originates in the neck from the brachiocephalic trunk. The left arises from the aortic arch in the thoracic region. The bifurcation into the external and internal carotid arteries occurs around the level of C4. The upper border of the internal carotid artery is the cranial part of the optic chiasm.

The resulting consensus delineation guidelines were depicted on 1 mm axial CT slices from an anatomy atlas in Mirada RTx (Mirada Medical Ltd., UK) (Supplemental material). The atlas in DICOM-RT format can be retrieved via the different co-operative groups.

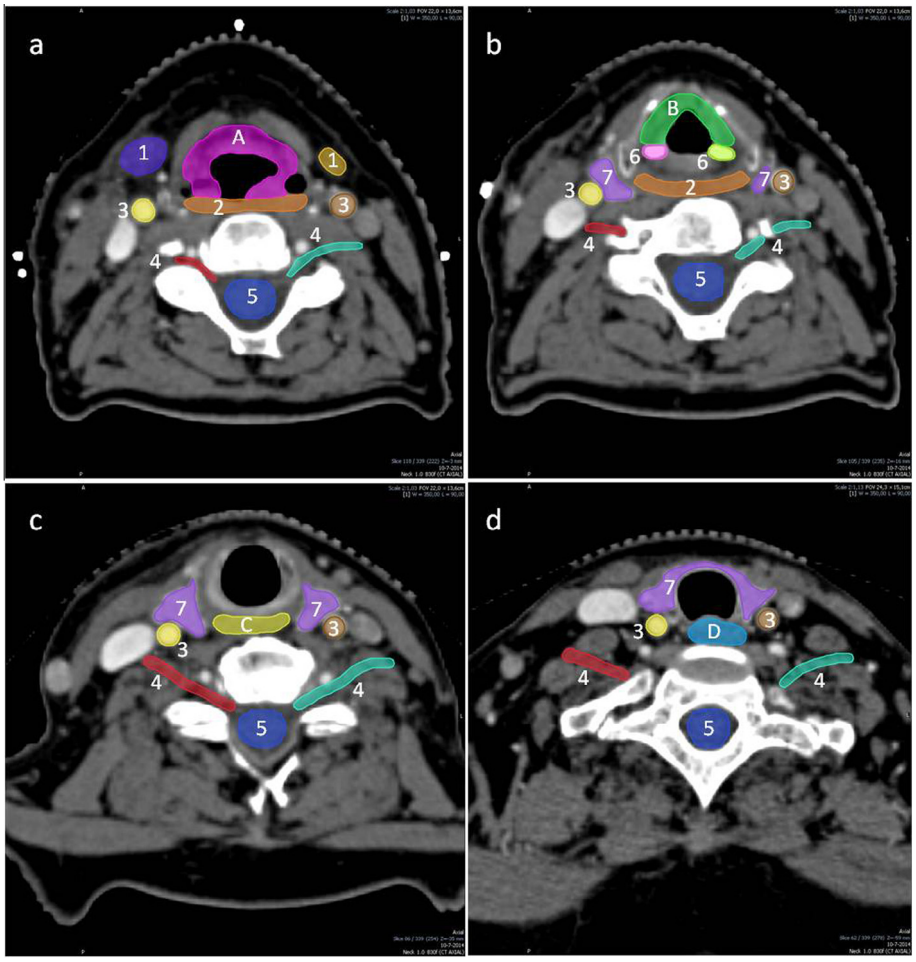

Fig. 4. Axial CT slices showing the delineation of the supraglottic larynx (A) (a), glottic area (B) (b), crico-pharyngeal inlet muscle (C) (c), and cervical esophagus (D) (d). Other organs at risks visible are the submandibular glands (1), pharyngeal constrictor muscles (2), carotid arteries (3), brachial plexus (4), spinal cord (5), arytenoids (6) and thyroid (7). (For the full atlas, the reader is referred to the Supplemental material.)

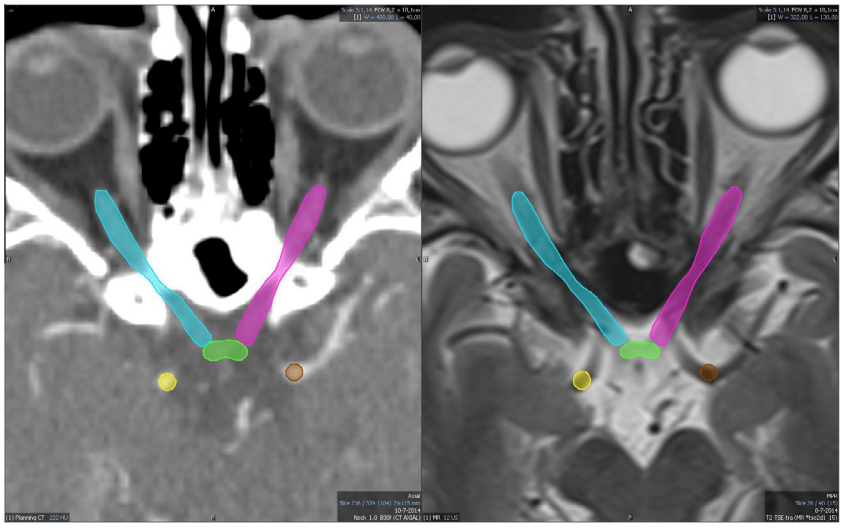

Fig. 5. Delineation of the optic nerves (blue and purple), optic chiasm (green) and carotid arteries (yellow and brown) on CT (left) and MRI-T2 (right).

Discussion

With the introduction of these consensus guidelines for delineation of OARs, we aim to decrease interobserver variability among clinicians and radiotherapy centers. These guidelines complement the previously published guidelines for neck node levels for head and neck tumors [1]. These two guidelines combined should contribute to reduce treatment variability and should also aid the design and implementation of multi-institutional clinical trials. The OAR guidelines are particularly useful when radiation-induced side effects are considered relevant endpoints. Moreover, the current consensus guidelines could facilitate the generalizability and clinical utility of Normal Tissue Complication Probability (NTCP) models.

We decided not to describe all possible OARs in great detail. Consequently, for some OARs we did not use single anatomic structures, but amalgamated surrogate structures involved in combined functions (e.g. the extended oral cavity). Nevertheless, the current guideline contains a comprehensive list of OARs. At the individual patient/center level one should decide which OAR to include, a decision that may depend on the tumor location, for example. In general, it is helpful to always include the delineation of the parotid and submandibular glands, spinal cord and PCM. For research purposes, OARs could be further subdivided (e.g. as described in case of the extended oral cavity, PCM, brainstem and brain).

There are natural variations for some OARs, such as the location of the bifurcation of the common carotid artery [21], which is used for contouring the brachial plexus. In addition, anatomic changes in OARs may occur due to tumor extension, or an OAR may be infiltrated by tumor. Therefore, a basic understanding of the normal anatomy remains essential.

For primary tumors of the nasopharynx, oral cavity and oropharynx, we strongly recommend the use of MRI in addition to CT. This will facilitate the delineation of OARs in this area, which includes the brainstem, spinal cord, pituitary gland, lacrimal glands, optic chiasm and optic nerves. MRI is ordinarily also beneficial for delineation of the parotid glands and PCM.

For primary tumors in close vicinity of the brain, we also recommend defining the temporal lobe and hippocampus (but delineation guidelines for these OARs are beyond the scope of these current guidelines) [15,16].

Some of the atlas structures are very small, such as the cochlea, pituitary gland, lacrimal glands and chiasm, with volumes <0.5 cm^3. Volume and dose–volume histogram (DVH) data calculated over such small volumes is susceptible to differences in the calculation algorithm (i.e. sampling and interpolation strategy), and also depend on CT slice thickness, pixel width, dose grid voxel width and DVH dose resolution, and may differ widely between the various methods [22]. Consequently we recommend expanding small structures such as the cochlea, pituitary gland, chiasm and arytenoids by 5 mm to calculate reliable and more consistent DVH data (but avoid overlap with the PTV). Additionally, we recommend acquiring constrast-enhanced CT scans with $\leqslant$2 mm slice thickness to improve delineations of such very small structures.

For some, serial OARs, ICRU recommends the addition of a PRV margin, which depends on planning technique and patient population [23]. For the spinal cord for example, it is common practice to add a 5 mm PRV margin [24]. In the case of OARs in close proximity to, or overlapping with the PTV, derived OAR structures can help to guide the planning process (i.e. OAR with subtraction of the PTV). For dose evaluation, however, the original OAR contour should be used. We advise to adhere to the standardized OAR naming conventions as proposed by Santanam et al. [25].

We recommend incorporating the current guidelines on a large scale to support consistent reporting of dose–volume data in addition to encouraging consistent radiotherapy practice for treatment prescriptions. Considering the increasing use and availability of MRI as well as the increasing knowledge and understanding about the OARs that are most relevant for side effects in radiotherapy, we anticipate updating these recommendations in the near future to a full MRI-based delineation guideline, incorporating as much anatomical and functional information as possible.

Conflict of interest statement

The authors declare no conflict of interest.

Acknowledgements

We would like to thank Biu Chan, MRT.T. (Princess Margaret, Toronto) for his expertise and recommendations on brachial plexus contouring.

Appendix A. Supplementary data

Supplementary data associated with this article can be found, in the online version, at http://dx.doi.org/10.1016/j.radonc.2015.07.041.

References

[1] Grégoire V, Ang K, Budach W, et al. Delineation of the neck node levels for head and neck tumors: A 2013 update. DAHANCA, EORTC, HKNPCSG, NCIC CTG, NCRI, RTOG, TROG consensus guidelines. Radiother Oncol 2014;110:172–81.
[2] Brouwer CL, Steenbakkers RJHM, van den Heuvel E, et al. 3D Variation in delineation of head and neck organs at risk. Radiat Oncol 2012;7:32.
[3] Brouwer CL, Steenbakkers RJHM, Gort E, et al. Differences in delineation guidelines for head and neck cancer result in inconsistent reported dose and corresponding NTCP. Radiother Oncol 2014:1–5.
[4] Steenbakkers RJHM, Duppen JC, Fitton I, et al. Observer variation in target volume delineation of lung cancer related to radiation oncologist-computer interaction: A "Big Brother" evaluation. Radiother Oncol 2005;77:182–90.
[5] Van de Water TA, Bijl HP, Westerlaan HE, et al. Delineation guidelines for organs at risk involved in radiation-induced salivary dysfunction and xerostomia. Radiother Oncol 2009;93:545–52.
[6] Hoebers F, Yu E, Eisbruch A, et al. A pragmatic contouring guideline for salivary gland structures in head and neck radiation oncology. Am J Clin Oncol 2013;36:70–6.
[7] Christianen MEMC, Langendijk JA, Westerlaan HE, et al. Delineation of organs at risk involved in swallowing for radiotherapy treatment planning. Radiother Oncol 2011;101:394–402.
[8] Dirix P, Abbeel S, Vanstraelen B, et al. Dysphagia after chemoradiotherapy for head-and-neck squamous cell carcinoma: dose-effect relationships for the swallowing structures. Int J Radiat Oncol Biol Phys 2009;75:385–92.
[9] Caglar HB, Tishler RB, Othus M, et al. Dose to larynx predicts for swallowing complications after intensity-modulated radiotherapy. Int J Radiat Oncol Biol Phys 2008;72:1110–8.
[10] Caudell JJ, Schaner PE, Desmond RA, et al. Dosimetric factors associated with long-term dysphagia after definitive radiotherapy for squamous cell carcinoma of the head and neck. Int J Radiat Oncol Biol Phys 2010;76:403–9.
[11] Feng FY, Kim HM, Lyden TH, et al. Intensity-modulated radiotherapy of head and neck cancer aiming to reduce dysphagia: early dose-effect relationships for the swallowing structures. Int J Radiat Oncol Biol Phys 2007;68:1289–98.
[12] Li B, Li D, Lau DH, et al. Clinical-dosimetric analysis of measures of dysphagia including gastrostomy-tube dependence among head and neck cancer patients treated definitively by intensity-modulated radiotherapy with concurrent chemotherapy. Radiat Oncol 2009;4:52.
[13] Schwartz DL, Hutcheson K, Barringer D, et al. Candidate dosimetric predictors of long-term swallowing dysfunction after oropharyngeal intensity-modulated radiotherapy. Int J Radiat Oncol Biol Phys 2010;78:1356–65.
[14] Hall WH, Guiou M, Lee NY, et al. Development and validation of a standardized method for contouring the brachial plexus: preliminary dosimetric analysis among patients treated with IMRT for head-and-neck cancer. Int J Radiat Oncol Biol Phys 2008;72:1362–7.
[15] Scoccianti S, Detti B, Gadda D, et al. Organs at risk in the brain and their dose-constraints in adults and in children: A radiation oncologist's guide for delineation in everyday practice. Radiother Oncol 2015;114:230–8.
[16] Sun Y, Yu X-L, Luo W, et al. Recommendation for a contouring method and atlas of organs at risk in nasopharyngeal carcinoma patients receiving intensity-modulated radiotherapy. Radiother Oncol 2014;110:390–7.
[17] Kocak-Uzel E, Gunn GB, Colen RR, et al. Beam path toxicity in candidate organs-at-risk: Assessment of radiation emetogenesis for patients receiving

head and neck intensity modulated radiotherapy. Radiother Oncol 2014;111:281–8.
[19] De Moraes CG. Anatomy of the visual pathways. J Glaucoma 2013; 22:S2–7.
[20] Celesia GG, DeMarco PJ. Anatomy and physiology of the visual system. J Clin Neurophysiol 1994;11:482–92.
[21] Ashrafian H. Anatomically specific clinical examination of the carotid arterial tree. Anat Sci Int 2007;82:16–23.
[22] Ebert MA, Haworth A, Kearvell R, et al. Comparison of DVH data from multiple radiotherapy treatment planning systems. Phys Med Biol 2010;55:N337–46.
[23] Bethesda, MD IC on RU and M. ICRU Report 62. Prescribing, Recording, and Reporting Photon Beam Therapy (Supplement to ICRU Report 50). 1999.
[24] Purdy JA. Current ICRU definitions of volumes: limitations and future directions. Semin Radiat Oncol 2004;14:27–40.
[25] Santanam L, Hurkmans C, Mutic S, et al. Standardizing naming conventions in radiation oncology. Int J Radiat Oncol Biol Phys 2012;83:1344–9.